Robotica (2022), **40**, pp. 120–135
doi:10.1017/S0263574721000424

CAMBRIDGE
UNIVERSITY PRESS

RESEARCH ARTICLE

A novel methodology to explore the periodic gait of a biped walker under uncertainty using a machine learning algorithm

Namjung Kim[1], Bongwon Jeong[2] and Kiwon Park[3,*]

[1]Department of Mechanical Engineering, Gachon University, Seongnam, South Korea, [2]Innovative SMR System Development Division, Korea Atomic Energy Research Institute, Daejeon, South Korea and [3]Department of Mechatronics Engineering, Incheon National University, Incheon, South Korea
*Corresponding author. Email: kiwon@inu.ac.kr

Received: 31 October 2020; **Revised:** 6 February 2021; **Accepted:** 27 March 2021; **First published online:** 28 May 2021

Keywords: bipeds, legged robots, uncertainty quantification, stability analysis, human biomechanics

Abstract

In this paper, we present a systematic approach to improve the understanding of stability and robustness of stability against the external disturbances of a passive biped walker. First, a multi-objective, multi-modal particle swarm optimization (MOMM-PSO) algorithm was employed to suggest the appropriate initial conditions for a given biped walker model to be stable. The MOMM-PSO with ring topology and special crowding distance (SCD) used in this study can find multiple local minima under multiple objective functions by limiting each agent's search area properly without determining a large number of parameters. Second, the robustness of stability under external disturbances was studied, considering an impact in the angular displacement sampled from the probabilistic distribution. The proposed systematic approach based on MOMM-PSO can find multiple initial conditions that lead the biped walker in the periodic gait, which could not be found by heuristic approaches in previous literature. In addition, the results from the proposed study showed that the robustness of stability might change depending on the location on a limit cycle where immediate angular displacement perturbation occurs. The observations of this study imply that the symmetry of the stable region about the limit cycle will break depending on the accelerating direction of inertia. We believe that the systematic approach developed in this study significantly increased the efficiency of finding the appropriate initial conditions of a given biped walker and the understanding of robustness of stability under the unexpected external disturbance. Furthermore, a novel methodology proposed for biped walkers in the present study may expand our understanding of human locomotion, which in turn may suggest clinical strategies for gait rehabilitation and help develop gait rehabilitation robotics.

1. Introduction

A passive biped walker is a simple mechanical system consisting of two legs connected by a joint. It was first developed in the early 1990s and has shown that a stable periodic gait down a slope can be produced without any external energy input when the appropriate initial conditions are applied [1]. During the swing phase, it acts as an inverted-joint pendulum with a single support. One of its major advantages is that it does not require any controllers or motors because its gait is spontaneously generated by gravity and inertia. This feature makes the biped walker energy efficient because the energy required to power a controller or actuate muscular activity is not required.

The biped walker is interesting because its periodic gait is remarkably similar to human locomotion [2]. Its governing equation consists of nonlinear ordinary differential equations combined with discrete switching conditions. Although the passive biped walker is mechanically simple, it contains a key characteristic of the dynamics of human walking. When the proper initial conditions are applied to a biped

walker, it walks down a slope with a periodic gait, which can be regarded as a "limit cycle" in the scope of dynamical systems with a two-dimensional phase plane [3]. The evolution of this limit cycle is a key characteristic of passive dynamic walking imitating the gait of a human.

While recent cutting-edge biped robots such as ASIMO [4] and HUBO [5, 6] seem to mimic the human gait at the glance, their mechanism of walking based on the zero moment point differs significantly from that of a human in many respects [7]. Thus, it is hard to gain insights into the mechanism of human walking by merely examining biped robots under dynamic control. In addition, understanding how humans walk directly from experiments is extremely difficult to achieve because of the complexity of the human central nervous system; the central nervous system regulates multiple body segments in a properly ordered fashion to repeat the gait under instability, which is not easily monitored. Due to these difficulties, the present study focuses on gait mechanics which consist of simultaneous movements of different body segments with minimal energy expenditure. In addition, it is necessary to explore a simple model that explains the essence of human locomotion: a passive biped walker. Unlike understanding the gait of ASIMO and HUBO, the profound understanding of a passive biped walker enables us to understand energy optimality, periodicity, and the stability of the human gait, in order to develop innovative prosthetic limbs and superior humanoid robot designs.

One of the main challenges in a passive biped walker is to evolve toward and maintain its stability during walking. This is not an easy task because of its intrinsic instability. In this study, we limit our interest of a biped walker's stability to two aspects: (1) choosing the appropriate initial conditions and (2) robustness against the external disturbances. The external disturbance used in this study implies various types of unexpected inputs in the real system such as obstacles, irregular surfaces, other people unexpectedly approaching, and physical force disturbances during gait. Previously, choosing initial conditions that could lead the biped walker's periodic gait were based on heuristics [8]. However, this approach examines only a limited region of parametric space as finding the appropriate initial conditions manually takes a considerable amount of time and money.

Even though the stability of gait is attained via the appropriate initial conditions, maintaining a stable gait is another challenge altogether, because of unexpected perturbations caused by external circumstances, such as positional and accelerative impacts. These unexpected external perturbations force the periodic gait out of its limit cycle, causing the biped walker to eventually collapse. In order to maintain gait stability while walking, the robustness of the biped walker against the external perturbations needs to be analyzed, so that its outcomes can then be used as guidelines for filtering any excessive external disturbances.

The purpose of this study is to propose a systematic approach that finds the appropriate initial conditions of a given biped walker using a recent machine learning technique, called particle swarm optimization (PSO) [9]. This agent-based optimization technique helps us to explore the search domain of initial conditions and finds multiple initial conditions that lead the biped walker stable while walking. In addition, the robustness of the biped walker is also examined in this study. A perturbation in position is generated from the probabilistic distribution to mimic an external disturbance and is applied to the biped walker to analyze the robustness of its stability. Several different locations in the limit cycle were chosen to analyze the uniformity of robustness in the periodic gait.

2. Materials and methods

2.1. Biped walker modeling

The biped walker has two rigid legs connected by a frictionless joint as shown in Fig. 1. The mass of the hip is usually much larger than that of the foot so that motion of the foot does not induce motion of the hip. As the leg hits the ground (surface of the slope) when the heel strikes, its velocity is set to zero instantaneously. We assumed there to be no-slip and no-bounce conditions at this moment.

https://doi.org/10.1017/S0263574721000424 Published online by Cambridge University Press

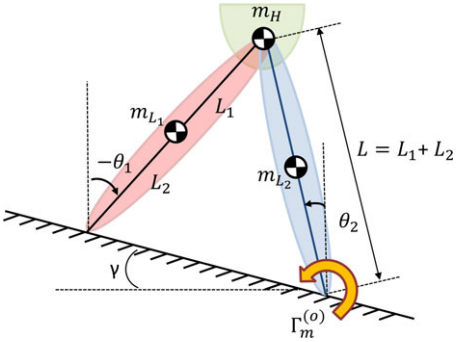

Figure 1. *Passive biped walking model.*

During walking, the fixed leg acts as a hinge and the other leg swings like an inverted pendulum, so that only one leg is in contact with the ground during the walking gait. The inclined angle of the slope is given as γ. The gait motion on the slope is generated by its inertia and gravity without any external effort. The motion of the biped walker is governed by the laws of classical rigid body motion. Several assumptions are made to simplify the dynamics of the biped walker as follows:

(1) The legs and the hip are considered to be lumped masses.
(2) The leg has a point foot that is connected to the ground without any slip or bounce during a complete step of the walking gait.
(3) During the heel strike, the configuration of the biped walker is unchanged.
(4) The swing leg only experiences an impact with the ground during the heel strike. This impact occurs instantaneously.

Given the assumptions regarding the biped walker, the equation of motion can be derived about the origin o as follows:

$$M(\Phi)\ddot{\Phi} + C\left(\Phi,\dot{\Phi}\right)\dot{\Phi} + K(\Phi) = 0 \tag{1}$$

where

$$\begin{aligned}
\Phi &= [\theta_1, \theta_2], \\
M(\Phi) &= \begin{bmatrix} p_1 & -p_2\cos(\theta_1 - \theta_2) \\ -p_2\cos(\theta_1 - \theta_2) & p_3 \end{bmatrix}, \\
C\left(\Phi,\dot{\Phi}\right) &= \begin{bmatrix} 0 & -p_2\dot{\theta}_2\sin(\theta_1 - \theta_2) \\ p_2\dot{\theta}_1\sin(\theta_1 - \theta_2) & 0 \end{bmatrix}, \\
K(\Phi) &= \begin{bmatrix} -p_4\sin(\theta_1) \\ p_5\sin(\theta_2) \end{bmatrix}.
\end{aligned} \tag{2}$$

M, C, and K are the mass, damping, and stiffness matrices of the biped walker. Φ is 1-by-2 matrix whose elements are θ_1 and θ_2, which are the angular positions of both legs. The time derivative is displayed as the dot in the equation. p_1 to p_5 are the physical parameters that are obtained from the physical characteristics of the biped walker. The detailed expressions are given as follows:

$$\begin{aligned}
p_1 &= m_H L^2 + m_L L^2 + m_L L_2^2, \\
p_2 &= m_L L L_1,
\end{aligned}$$

https://doi.org/10.1017/S0263574721000424 Published online by Cambridge University Press

$$p_3 = m_L L_1^2,$$
$$p_4 = (m_L L_2 + m_L L + m_H L)g,$$
$$p_5 = m_L L_1 g, \tag{3}$$

where g is the gravitational acceleration. The masses of the system are modeled by using m_H and m_L, which correspond to the effective mass of the hip and the leg, respectively. The location of the mass from of the foot and from of the hip is defined as L_1 and L_2, respectively. The length of the legs, L, is defined as the summation of L_1 and L_2.

This system of second-order differential equations consists of two coupled differential equations that represent the angular momentum conservation with respect to the foot (for the whole mechanism) and the hip (for the swinging leg), respectively. The equation of motion describes the continuous dynamics of the biped walker during the walking period. To describe the instant impact during the heel strike, an impact map must be formulated to prevent intersection between the leg and the ground.

When the swing leg impacts the surface of the ground, a discrete input from the ground exists that induces a jump of the angular velocities $\dot{\theta}_1$ and $\dot{\theta}_2$. This discrete jump can be formulated as a sudden transition between the velocities just before and after collision with the ground:

$$\begin{bmatrix} \dot{\theta}_1^+ \\ \dot{\theta}_2^+ \end{bmatrix} = \Delta(\Phi) \begin{bmatrix} \dot{\theta}_1^- \\ \dot{\theta}_2^- \end{bmatrix} \tag{4}$$

The – and + signs denote the instant in time before and after the impact, respectively. As described before, the angular momentum before and after the impact is assumed to be conserved as the impact force is the only external force affecting the biped walker and is exerted on the origin of the angular momentum. The angular momentum on the origin, $\Gamma_m^{(o)}$, is as follows:

$$\Gamma_m^{(o)} = \sum_i r_i^{(o)} \times m_i v_i^+ = \sum_i r_i^{(o)} \times m_i v_i^-, \; i \in \{L, H\} \tag{5}$$

where the reference point is denoted as *(o)* in Fig. 1, and the position vector $r_i^{(o)}$ relative to this point is given as

$$r_{L_2}^{(o)} = \begin{bmatrix} -L_2 \sin(\theta_1) \\ L_2 \cos(\theta_1) \\ 0 \end{bmatrix},$$
$$r_{L_H}^{(o)} = \begin{bmatrix} -L \sin(\theta_1) \\ L \cos(\theta_1) \\ 0 \end{bmatrix},$$
$$r_{L_1}^{(o)} = r_{L_H}^{(o)} + \begin{bmatrix} -L_1 \sin(-\theta_2) \\ -L_1 \cos(-\theta_2) \\ 0 \end{bmatrix}. \tag{6}$$

In Eq. (6), v_i^- and v_i^+ are the velocities before and after impact, respectively. The velocities can be obtained from the following:

$$v_H^- = \begin{bmatrix} 0 \\ 0 \\ \dot{\theta}_2^- \end{bmatrix} \times \begin{bmatrix} L \sin(-\theta_2) \\ L \cos(-\theta_2) \\ 0 \end{bmatrix}, \; v_H^+ = \begin{bmatrix} 0 \\ 0 \\ \dot{\theta}_1^+ \end{bmatrix} \times \begin{bmatrix} -L \sin(-\theta_1) \\ L \cos(-\theta_1) \\ 0 \end{bmatrix},$$

https://doi.org/10.1017/S0263574721000424 Published online by Cambridge University Press

$$v_{L_1}^- = \begin{bmatrix} 0 \\ 0 \\ \dot{\theta}_2^- \end{bmatrix} \times \begin{bmatrix} L_2\sin(-\theta_2) \\ L_2\cos(-\theta_2) \\ 0 \end{bmatrix},\ v_{L_1}^+ = v_H^+ + \begin{bmatrix} 0 \\ 0 \\ \dot{\theta}_2^+ \end{bmatrix} \times \begin{bmatrix} -L_1\sin(-\theta_2) \\ L_1\cos(-\theta_2) \\ 0 \end{bmatrix},$$

$$v_{L_2}^- = v_H^- + \begin{bmatrix} 0 \\ 0 \\ \dot{\theta}_1^- \end{bmatrix} \times \begin{bmatrix} L_1\sin(\theta_1) \\ -L_1\cos(\theta_1) \\ 0 \end{bmatrix},\ v_{L_2}^+ = \begin{bmatrix} 0 \\ 0 \\ \dot{\theta}_1^+ \end{bmatrix} \times \begin{bmatrix} -L_2\sin(\theta_1) \\ L_2\cos(\theta_1) \\ 0 \end{bmatrix}. \tag{7}$$

By substituting Eqs. (6) and (7) into Eq. (5), we can obtain the equation of motion for the biped walker. The equation can be obtained by considering the geometrical constraints of the biped walker. When the two legs instantaneously contact the surface of the ground, there exists an additional constraint that correlates the geometrical parameters of the biped walker with the angle of the slope:

$$\cos(\gamma + \theta_1) - (\gamma + \theta_2) = 0 \tag{8}$$

Once the dynamics of the biped walker and the constraints are set, the stability of the gait needs to be characterized. The concept of gait stability as applied to walking behavior is hard to define but is crucial for the performance analysis of the system. The conventional definition of the stability of a system (i.e., Lyapunov stability) around an equilibrium point is not suitable for such systems, given that (1) the dynamic characteristics of these system are typically represented by the periodic orbits rather than a set of points of interests, and (2) these systems intrinsically bear discontinuities induced by the heel-strike impact; hence, we define the stability of a system in terms of its orbital stability [3]. It is natural to suggest that a gait is stable if, starting from a steady closed phase trajectory, any finite disturbance leads to another nearby trajectory of similar shape [10]. Furthermore, if, in spite of the disturbance, the system returns to the original cycle, the gait is called asymptotically stable [10]. For certain initial conditions, the contour of the biped walker passes the same path on the phase plot. Therefore, this problem can be considered to be the finding of the initial conditions that minimize the deviation between the previous and current contour path in the phase plot as the gait evolves, and the motion satisfies its geometrical constraints [11].

2.2. Multi-objective, multi-modal particle swarm optimization

As we described in the previous section, finding the appropriate initial conditions that enable the biped walker to remain in its periodic gait can be considered to be finding an optimal initial velocity and position that minimizes the distance deviations between gait cycles while satisfying the walker's geometrical constraints. As obtaining the periodic gait of the biped walker involves many parameters and its dynamics can easily change owing to small changes in the initial conditions, we can expect the response surface in a search space to be extremely nonlinear. Traditional gradient-based optimization algorithms often fail to find optimized solutions to these kinds of problems, which is why searching for the suitable initial conditions for periodic gait so easily fails or is so time-consuming.

Recently, various population-based optimization techniques, such as the genetic algorithm, [12] PSO, [9] and ant colony optimization, [13] have garnered attention because of their derivative-free characteristics and efficiency. PSO is one of the population-based optimization algorithms that mimic the social behavior of birds or fish. Each member of the flock, called an agent, is distributed randomly in the search space when the algorithm starts. As the iteration increases, it evolves toward the global optimizer based on its and its neighbor's experiences. The experience of each agent, here, represents the evolution of a solution that converges toward the global optimizer. PSO has become popular because of the following distinctive advantages [14]: (1) generality, (2) usability, and (3) computational efficiency. However, PSO is not a proper method to solve the MOMM optimization problems because PSO defines only one agent, called a leader, which has the best cost function value at the certain iteration: the other agents tend to converge to the leader. As iteration proceeds, if the agent that has the better cost function value than

https://doi.org/10.1017/S0263574721000424 Published online by Cambridge University Press

```
BEGIN
    Initialize all agents' velocity and position
    Initialize personal best archive (PBA) and its neighbor' best archive (NBA)
    Iteration = 0
    WHILE iteration < threshold
      FOR each agent, i
        Sort the non-dominated agents in PBA_i and NBA_i using non-dominated-scd-sort-algorithm
        Select personal best (PBEST_i) and its neighbor's best (NBEST_i) from sorted PBA_i and NBA_i
            PBEST_i = first agent in sorted PBA_i
            NBEST_i = first agent in sorted NBA_i
        Update agent's velocity and position
        Update PBA_i and remove dominated agents in PBA_i
      FOR each agent, i
        Update NBA_i using PBA_i
    END
    Output the non-dominated agents in all NBA
END
```

Figure 2. *Pseudo-code for multi-objective multi-model particle swarm optimization.*

the leader, the leader is replaced. PSO is a powerful method to solve the optimization problem, but it is limited to locate only one global minimum because of the way to define the leader.

In this study, we are interested in PSO to solve our MOMM optimization problem. This is important for us because (1) our problem has two objective functions (geometrical constraints and distance deviation in the limit cycle) and (2) multiple initial conditions that result in the same objective function value might exist.

One of the most popular techniques to expand the solvability of PSO for MOMM optimization problems is the niching technique [15]. The basic idea of the niching technique is to limit each agent's searching area properly so that all agents converge to the multiple local minima instead of one global minimum. Several variations of such niching methods have been proposed [16, 17, 18, 19]; however, these niching techniques involve a relatively large number of parameters, such as the sharing radius or crowding factors. These parameters are often difficult to set, and the generality of PSO is lost because they depend on the characteristics of each optimization problem. In this study, we used a variation of PSO using a ring topology and a SCD as proposed by Yue et al., [20] which can form stable niches without any niching parameters. We used the source code available in the public domain and modified it to meet our requirements. A brief description of the algorithm is shown in Fig. 2, and a detailed guideline of its usage is explained in a previous study [20].

First, the algorithm initializes the agents' positions and velocities. For the initial step, all agents are started at a randomly selected position and velocity. The personal best archive (PBA_i) is a memory that stores ith agent's best experience along its evolution path. The neighbors' best archive (NBA_i) is a memory that stores ith agent's neighbor's best experience during the evolution. Both the PBA_i and NBA_i memories are initialized at the beginning.

During the evolution, the PBA_i and NBA_i are sorted using a non-dominated sorting algorithm [20]. The sorting algorithm is one of the most important features in MOMM optimization algorithms in two respects: (1) the selection of a leader; (2) the management of the agent's distribution. For a simple PSO, the leader is an agent that has a minimum objective value based on each agent's history and all agent's objective values in the current iteration. This is straightforward as in each iteration, there exists one leader.

However, for the multi-objective problem, each agent produces two or multiple objective values that might be in conflict with each other. Therefore, a set of agents should be selected such that the agents minimize the multiple objective functions simultaneously. This is called a Pareto set [21]. For multi-modal problems, even if the objective value is the same, there is a possibility that multiple agents at different locations produce the same objective value. These issues can be solved by choosing a sorting algorithm

https://doi.org/10.1017/S0263574721000424 Published online by Cambridge University Press

with careful limiting neighbors. In this study, a specific sorting algorithm called a non-dominated-special-crowding-distance-sorting algorithm (non-dominated-scd-sort algorithm) is employed to limit the number of neighbors properly [22].

The non-dominated-scd-sort algorithm consists of two steps: (1) sorting agents using a non-dominated sorting scheme and (2) selecting agents within a SCD. The non-dominated agent stands for the agent that does not have an upfront agent in the objective space. This means that this agent can be a candidate of the optimizer. The SCD is a specific distance measure that controls an agent's densities in the decision space and objective space. The decision space is the space that is defined by variables that need to be optimized. The objective space is the space where each axis corresponds to each objective function. Selecting the proper SCD for each agent enables the location of all agents in multiple local minima. Using two steps, the non-dominated agents are ranked in the descending order according to their SCD, so that multi-modal solutions in the Pareto optimal set are found efficiently using this algorithm.

After sorting, the best experience of ith agent and its neighbors' best experiences are chosen as the personal best ($PBEST_i$) and its neighbors' best ($NBEST$). Then, the agent's position and velocity are updated according to the following equations:

$$\begin{aligned} \underline{x}_i(t) &= \underline{x}_i(\mathrm{t}-1) + \underline{v}_i(t), \\ \underline{v}_i(t) &= \mathrm{k}\underline{v}_\mathrm{i}(t-1) + C_1 r_1(\underline{x}_{PBEST,i} - \underline{x}_i(t)) + C_2 r_2(\underline{x}_{NBEST,i} - \underline{x}_i(t)), \end{aligned} \tag{9}$$

where k is inertia weight, $\underline{v}_i(t)$ and $\underline{x}_i(t)$ denote velocity and position of an agent i, at time t, respectively. If k increases, the direction of evolution is similar to that of the previous step; otherwise, the direction of evolution proceeds toward the personal or the neighbor's best. The underscore indicates that the velocity and position are n-dimensional vectors, where n is the number of optimizing parameters. r_1 and r_2 are random values, uniformly sampled in [0,1], that provide randomness of search direction. C_1 and C_2 are constants, called cognitive and social learning factors, respectively. These constants define the amount of attraction toward the agent's own best experience or that of its neighbors. $\underline{x}_{PBEST,i}$ is the best position that the agent i experiences and $\underline{x}_{NBEST,i}$ is the best position of its neighbor. By choosing the right neighbor and balancing the terms related to C_1 and C_2, the algorithm enhances the ability to search for the optimum in the search space.

After updating all agents' PBA, the memory of ith agent's neighbor, NBA_i, is updated using the updated PBA. The updated NBA_i is selected as the non-dominated agents in the PBA of ith agent's neighbors. The updating procedure is repeated until the iteration reaches the threshold, which is defined as the maximum number of iterations. The Pareto set that contains the solutions of MOMM optimization problem is the non-dominated agents in the NBA when the iteration ends.

3. Results and discussion

3.1. Characteristics of periodic gaits

Inspecting several outputs from the walker help us to understand the characteristics of periodic gait. Figure 3 shows the phase trajectory of the biped walker and four instant markers (I–IV) display the moments when the biped walker changes its phase. The instant marker I corresponds to time $t = 0^+$, the instant moment after the rear and the swing legs are contacted with the ground ($t = 0$). Then, the rear leg that was contacted with the ground, supporting the walker in the previous step, loses contact with the ground and becomes the swing leg. The stick diagram shows a red leg as a swing leg and blue leg as a rear leg. As the walker moves, the phase trajectory evolves in the clockwise approaching to the instant marker II in this diagram as shown by the arrowheads. During the upper half of the cycle (I→II), the walker behaves like a simple pendulum centered at the hip position. The instant marker II corresponds to time $t = T^-$, the instant moment before the swing leg contacts with the ground ($t = T$). After passing the moment $t = T$ when the rear leg and the swing leg were contacted with the ground together (the instant moment III), the swing leg becomes the supporting leg. During the lower half of the cycle (III→IV),

https://doi.org/10.1017/S0263574721000424 Published online by Cambridge University Press

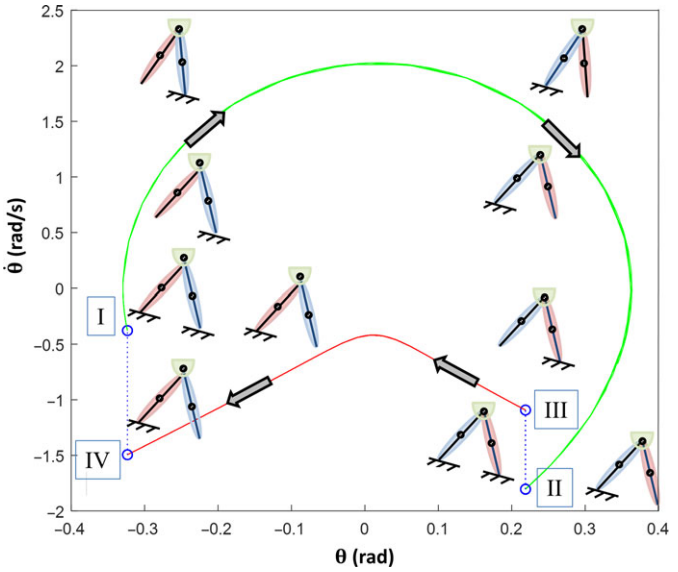

Figure 3. *Phase portrait of the biped walker in periodic gait.*

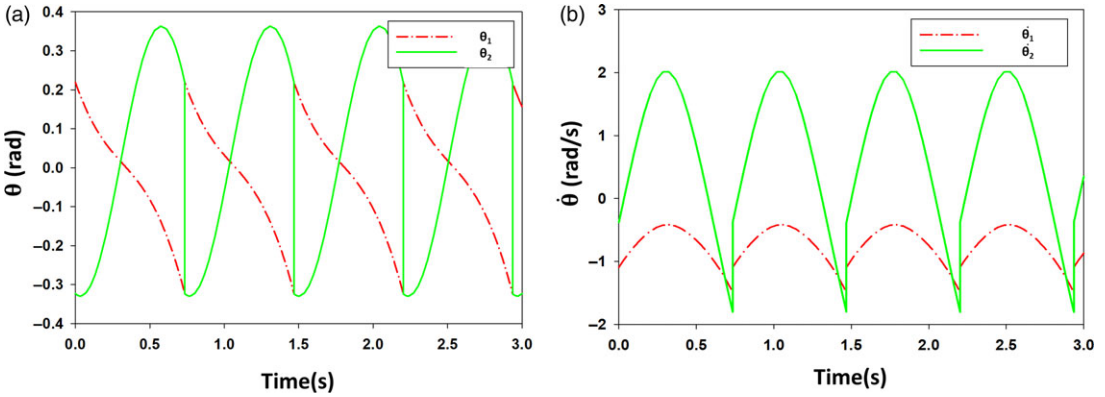

Figure 4. *Phase portrait of the biped walker in periodic gait.*

the motion of biped walker is described as an inverted pendulum hinged at the point of support. The velocity jumps at the moments IV→I and II→III are originated from the impact occurred at the leg from the ground.

Figure 4 shows the evolution of the angles of the stance (θ_1) and swing leg (θ_2) during the walking phase. This agrees with the initial assumption imposed when modeling the biped walker, that the impact forces are impulsive. The velocities $\dot{\theta}_1$ and $\dot{\theta}_2$ are discontinuous at impact due to the distinctive impact map describing the jump between θ^- and θ^+. These discontinuities are a direct consequence of the impact forces the biped walker experiences during heel strike with the slope. Without such forces, the biped would simply fall through the floor during the motion. The paths of θ_1 and θ_2 as well as $\dot{\theta}_1$ and $\dot{\theta}_2$ are periodic between nearby impacts, which represent the periodic gait of the biped walker.

Figure 5 shows the time between consecutive steps of the gait after each step of the cycle. It can be seen that the half-step period converges to T at ~ 0.734 when the gait is observed to be stable; it also infers that the initial condition is off within a certain range, and the time step eventually converges to T at ~ 0.734.

https://doi.org/10.1017/S0263574721000424 Published online by Cambridge University Press

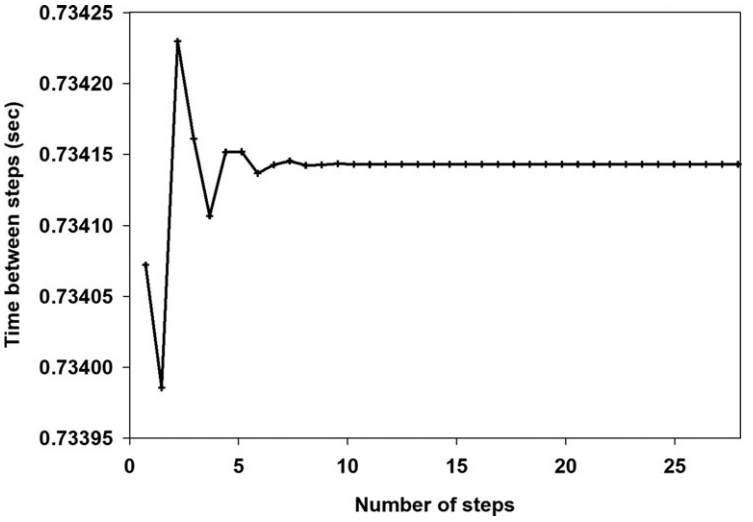

Figure 5. *Time between steps of the biped walker in periodic gait.*

3.2. Searching for periodic gait using MOMM-PSO

The population-based optimization approach with the conventional search technique, called MPMM-PSO, was used to find the proper initial conditions, which create a stable gait. The incline angle $\gamma = 3.0°$ was chosen in this study to verify the consistency of the result found using the proposed approach with the one given in a previous study [11]. The existence of the periodic gaits of the biped walker for a slope with angles between 0° and 4.4° was verified in another study [3]. The given initial condition for the stable periodic gait when $\gamma = 3.0\,°$ was $q_1 = 0.2169$ and $\dot{q_1} = -1.0848$ [11]. The physical parameters for the biped walker are given in Table 1.

Figure 6 shows the response values from geometrical constraints and the Euclidean distance of the limit cycle when the various q_1 and $\dot{q_1}$ were applied. The upper and lower values of q_1 and $\dot{q_1}$ were selected to be large enough to cover all feasible choices of the initial conditions. The traces of all agents were collected and displayed in the figure. Each point corresponds to the dynamics of the biped walker with given initial conditions. The colors of each point correspond to the Euclidean distance in the phase plot between the initial step and the time after three steps in order to confirm that the walker was in its periodic gait. The Euclidean distance higher than a certain limit was projected on the predefined maximum value, 5, for clear visibility in the figure.

The gaits of 13 different locations in the search domain were selected to analyze the behavior of the biped walker. The initial condition given at each location is shown in Table 2.

To confirm the gait stability of the biped walker with respect to the given initial condition, the dynamics of several cases are shown in Fig. 7. Some of the selected points show the fluctuations in several initial steps; however, the gait converged to the stable phase. Among the 13 locations, 3 locations (index 1, 5, 10) lead the biped walker in a periodic gait. Apart from index 1 (location analogous to the ref. [11]), there were two more locations that created a periodic gait in the biped walker. We selected several additional locations that existed on the line that connected the index 5 and 10 and analyzed the behavior of the biped walker, as shown in Fig. 8. Although the transient behaviors were somewhat different depending on the given initial conditions, all cases that lay on the line between index 5 and 10 converged to a periodic gait. This further confirmed that there existed multiple initial conditions leading the biped walker to periodic gaits. This was also an important finding in our research since conventional searching algorithms can only locate one initial condition for the periodic gait [11].

In addition to the dynamics of the periodic gaits of the biped walker, we investigated the major limiting factor of the stability of the biped walker by examining the details of the objective function. The objective

https://doi.org/10.1017/S0263574721000424 Published online by Cambridge University Press

Table 1. *Physical parameters of the biped walker.*

Hip mass (m_H)	10 kg
Stance leg (m_{L_1})	5 kg
Swing leg (m_{L_2})	5 kg
Location of the mass from the foot to center of mass of leg (L_1)	0.5 m
Location of the mass from the hip to center of mass of leg (L_2)	0.5 m

Table 2. *Initial conditions at the locations selected in Figure 6.*

Index	1	2	3	4	5	6	7	8	9	10	11	12	13
θ_1	0.219	0.219	0.219	0.219	0.200	0.180	0.165	0.200	0.200	0.165	0.165	0.165	0.102
$\dot{\theta_1}$	−1.092	−1.000	−.0921	−0.890	−1.092	−1.092	−1.092	−0.870	−0.800	−0.910	−0.740	−0.670	−1.686

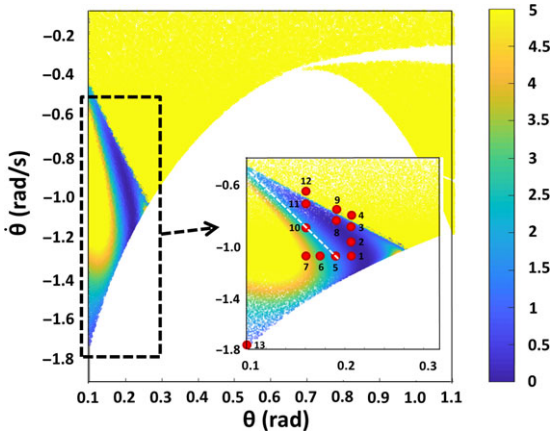

Figure 6. *Objective function values of the biped walker in a gait cycle.*

function was divided into two factors (geometrical constraints and distance deviations in a gait cycle), and its calculated values are shown in Fig. 9(a) and (b).

The colors in Fig. 9(a) and (b) depict the mismatch of geometrical constraints and distance deviation of the gait cycle, respectively. As shown in Fig. 9(a) and (b), the initial conditions that satisfied the geometrical constraints densely located in the limited domain compared to the case in the distance deviation of the gait cycle; this defied our initial intuition that the distance deviation generated by the gait cycle would be a major factor that limited the initial condition. This figure shows that satisfying the geometrical constraint, originating from the geometry of the walker, is the critical limiting factor for the stable initial condition.

3.3. Periodic gaits under uncertainty

In the previous section, the periodicity and stability of the biped walker were investigated with respect to different initial conditions. To further understand the stability of the biped walker, we now consider the dynamics of the biped walker under the external uncertainty while walking down the slope. The biped walker can be exposed to various external circumstances, including disturbances such as directional impacts in angular position, velocity, and sudden increases or decreases of mass. Even if the biped walker is set in a periodic gait by carefully choosing the proper initial conditions, it easily falls and becomes unstable when exposed to external impact. Therefore, it can be deduced that these external circumstances are closely related to the sustainability of the biped walker's periodic gait. In this study,

https://doi.org/10.1017/S0263574721000424 Published online by Cambridge University Press

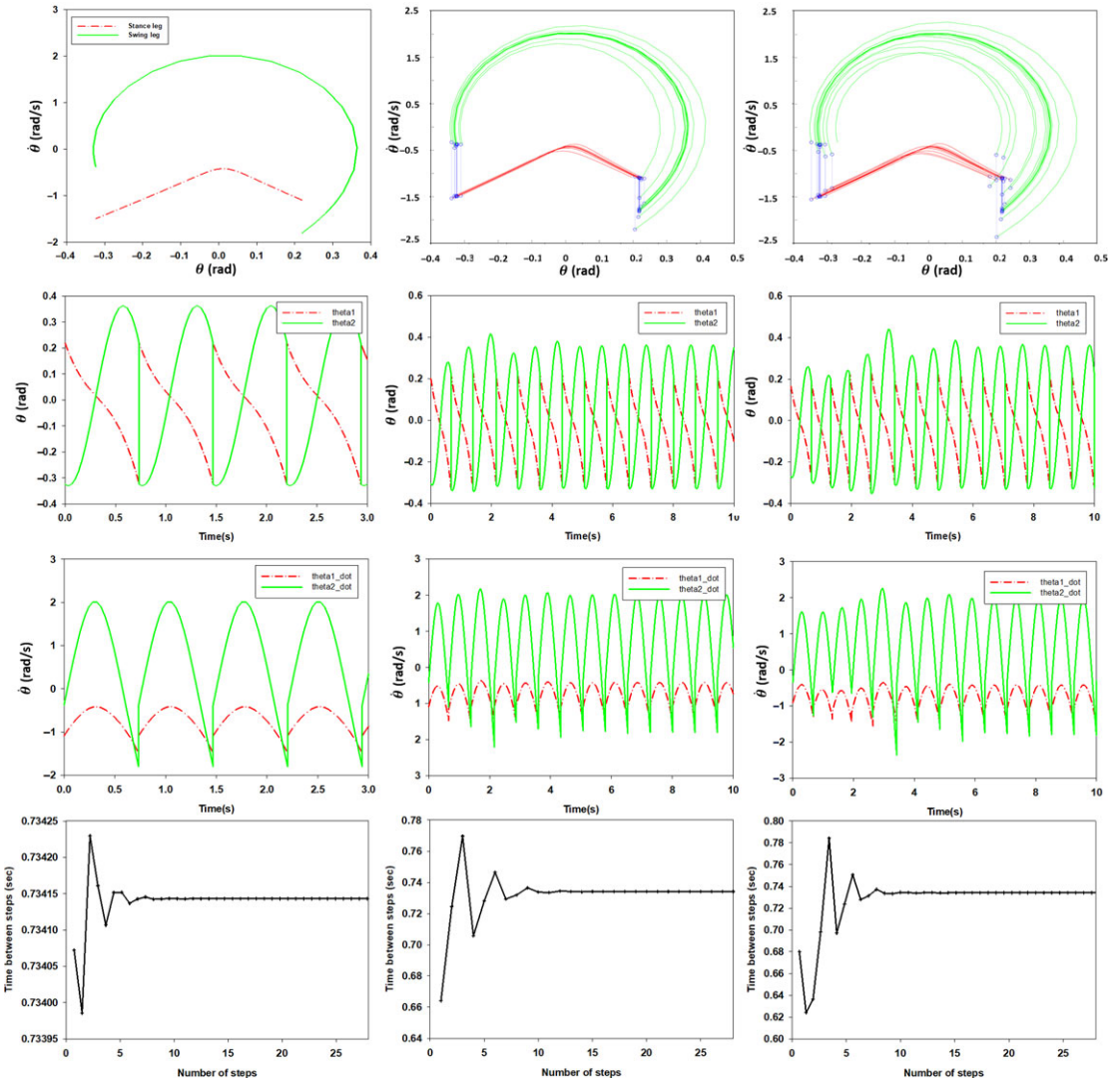

Figure 7. *Dynamic behavior of the biped walker that converges to periodic gaits: left index 1; middle: index 5; right: index 10 in Table 2.*

we limit our interest on the uncertainties in the angular position of the biped walker when it is in a periodic gait. Nine representative locations of the impacts were chosen and applied only on the swing leg, thereby limiting the allocation of uncertainties. This is based on the idea that the swing leg is exposed to the external impacts more often than the standing leg. Nevertheless, it should be noted that the same approach could easily be expanded to uncertainties in the standing leg too.

Figure 10 shows the phase plot of the biped walker in a periodic gait and nine locations where the external impact was applied. The physical parameters of the biped walker were identical to Table 1 and the slope angle γ was 3.0°. Nine impact locations (from LOC1 to LOC9) exist from the moment when the swing begins to the swing prepares the next step.

First, the biped walker walked a few steps with the given initial conditions leading to a periodic gait. After a few steps, an external impact was applied to the angular position (θ). The external impact was

https://doi.org/10.1017/S0263574721000424 Published online by Cambridge University Press

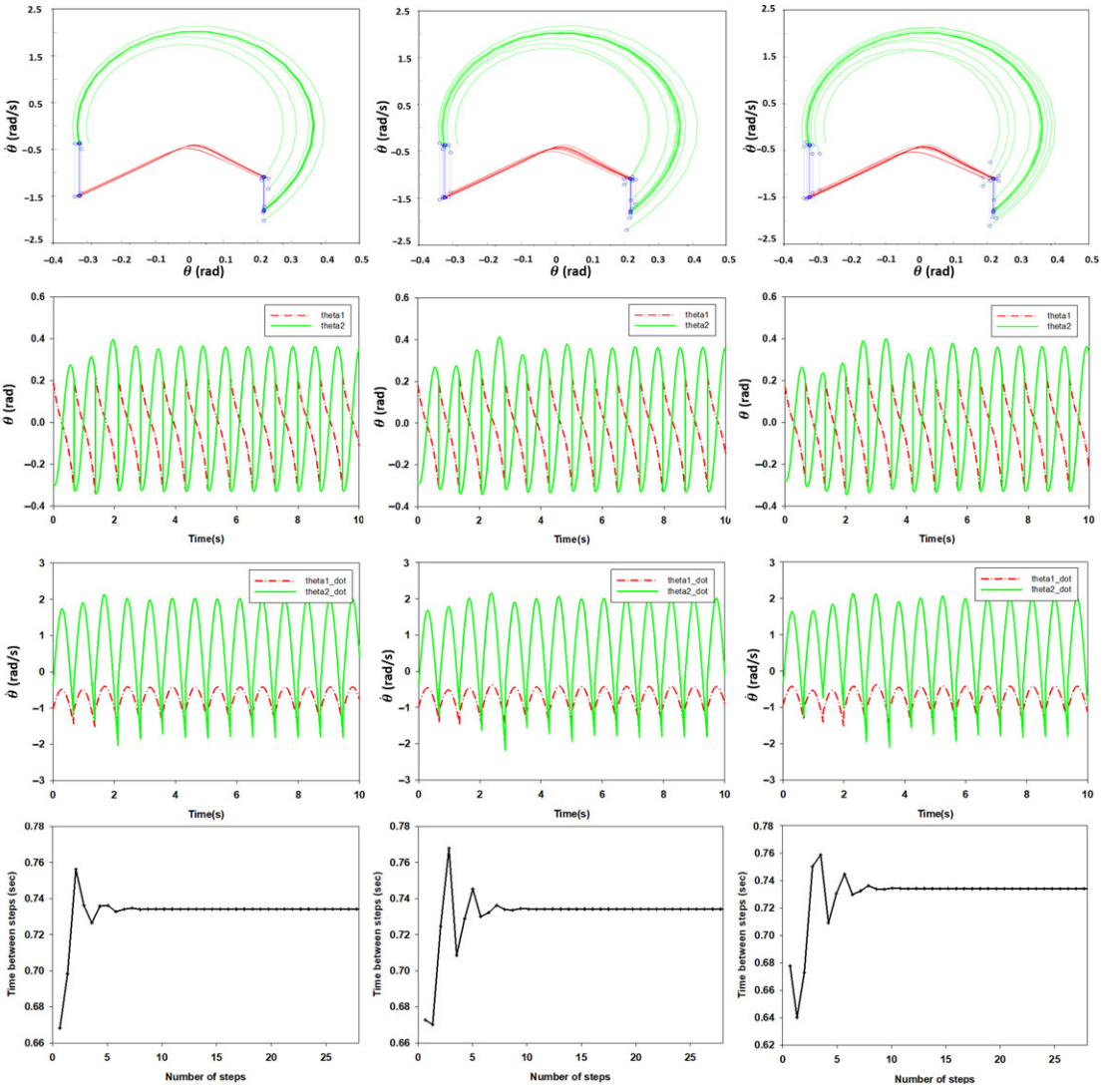

Figure 8. *Dynamic behavior of the biped walkers with three selected initial conditions that lie between index 5 and 10 in Table 2.*

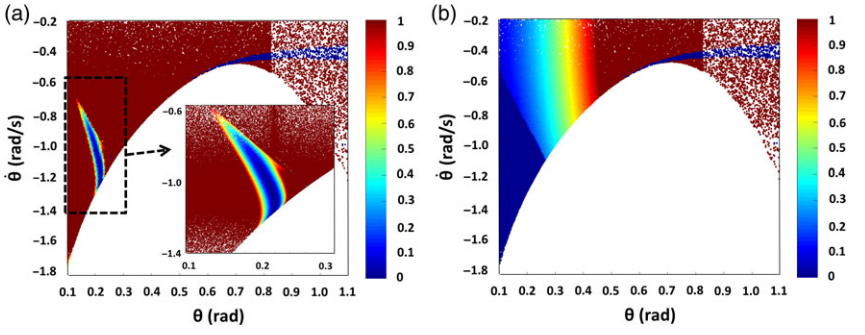

Figure 9. *Objective function values from (a) geometrical constraints and (b) distance deviation in a gait cycle.*

https://doi.org/10.1017/S0263574721000424 Published online by Cambridge University Press

Table 3. *Nine locations where the external impacts applied.*

Location	1	2	3	4	5	6	7	8	9
θ	−0.329	−0.319	−0.284	−0.215	−0.157	−0.0470	0.19	0.291	0.34
$\dot{\theta}$	−0.0738	0.490	0.990	1.490	1.74	1.99	1.744	1.229	0.722

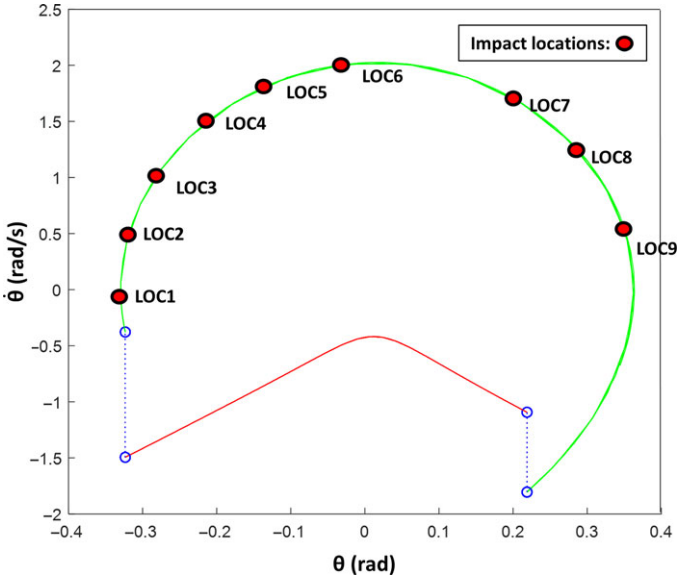

Figure 10. *Phase plot with nine impact locations for external uncertainties.*

generated using a normal distribution with zero mean and standard deviations 0.1. Table 3 describes locations where the impacts occurred.

Figure 11 shows the given external uncertainties and the stability of the biped walker with given uncertainties. The orange histogram shows the given impacts following the normal distribution. The blue and red points show the stable and unstable gait as a result of the given impacts, respectively.

As shown in Fig. 11, the stability of the gait depends on the magnitude of the external impact. This agrees well with our expectation that a larger impact would make the biped walker more unstable. However, what is unexpected in this result is that the robustness of the biped walker to the external impact was different depending on the direction in which the swing leg moved and the relative magnitude of the angular position. When the walker was in the negative angular position (from LOC1 to LOC6), the walker was more stable in the face of the positive positional impact (tolerable up to approximately 0.2 rad positional impact) than in the negative positional impact direction (up to approximately −0.1). On the other hand, when the walker was in the positive position (from LOC7 to LOC9), the walker was more stable to the negative positional impact (tolerable up to approximately −0.3 rad positional impact) than the positive positional impact direction (up to approximately 0.15). This inequality in the magnitude of maximum impact in the positive and negative directions suddenly changed as the impact location changes from the negative to the positive (LOC6 → LOC7). We infer that this asymmetry of the stable region about its central point (i.e., zero perturbation) can be attributed to the accelerating direction of the inertia. When the acceleration was increasing from LOC1 to LOC6, the positive perturbation served as an additive force contributing to the incremental acceleration, whereas the negative perturbation acted as an obstacle interfering with the smooth movement of the whole body. The opposite was observed from LOC7 to LOC9, where the negative perturbation was aligned well with the decremental acceleration.

https://doi.org/10.1017/S0263574721000424 Published online by Cambridge University Press

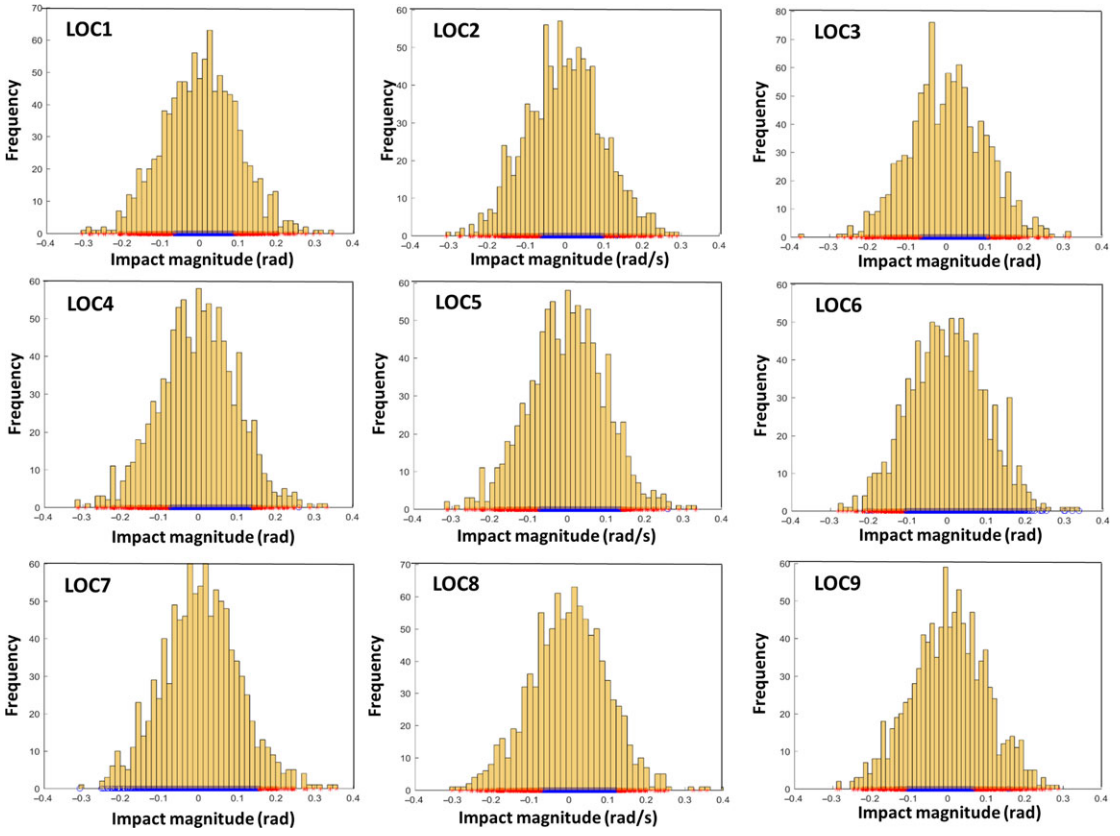

Figure 11. *Given external uncertainties and stability of the biped walker in nine locations. Blue and red points stand for the stable and unstable gaits after impact, respectively.*

Another noteworthy observation in Fig. 11 is that the maximum magnitude of uncertainties tolerable to the biped walker stable changed significantly depending on the impact location. This result is well aligned with previous reports showing a limit cycle of the biped walker surrounded by a basin of attraction, [23] where the fluctuating regions of the stability and instability for each point of the interest in the limit cycle has been demonstrated. Although we limited our current study to nine representative points, one can easily deduce that the expansion of the set points of interest will lead to the complete mapping of the sensitivity of each point to the external perturbation in the limit cycle. Based on the generated map, the robustness of the biped walker can be enhanced by lowering the sensitivity of the weak points via the parametric study, and the minimum tolerance of the external perturbation that ensures the robustness of the biped walker can also be identified. To demonstrate this hypothesis, further study is currently under investigation by the authors' research group.

4. Conclusions

A simple biped walker model representing the human walking gait was implemented, and model parameters were chosen based on previous studies. A meta-heuristic population-based optimization algorithm (MOMM-PSO) was used to obtain the appropriate initial conditions that lead to the biped walker exhibiting a stable gait. The results showed that the proposed approach could find multiple initial conditions, which could not be found using previous heuristic approaches. In contrast to the previous studies examining limit cycles of passive walkers, the present study investigated the robustness of stability of

https://doi.org/10.1017/S0263574721000424 Published online by Cambridge University Press

passive walkers when unexpected external forces were applied. The external disturbances were sampled from the probabilistic distributions, modeling the unexpected external impacts in angular positions while the biped walker was walking. The results from this study showed that the robustness of stability might change depending on the location of the impact, so that the maximum magnitude of impact that induces instability of gait may be different depending on where the impact is applied in the phase diagram. The proposed systematic approach presented in this study provides insight into the dynamic characteristics of the biped walker in terms of stability and the physiological motor control of human locomotion.

Funding. This work was supported in part by the National Research Foundation of Korea (NRF) grant funded by the Korea government (MSIT) (No. 2018R1C1B5086542).

Conflicts of Interest. The authors declare that there is no conflict of interest.

References

[1] T. McGeer, "Passive dynamic walking," *Int. J. Rob. Res.* **9**(2), 62–82 (1990).
[2] S. H. Collins, M. Wisse and A. Ruina, "A three-dimensional passive-dynamic walking robot with two legs and knees," *Int. J. Rob. Res.* **20**(7), 607–615 (2001).
[3] A. Goswami, B. Thuilot and B. Espiau, "Compass-like biped robot part I: Stability and bifurcation of passive gaits," (INRIA: Technical Report, 1996).
[4] Y. Sakagami, R. Watanabe, C. Aoyama, S. Matsunaga, N. Higaki and K. Fujimura, "The Intelligent ASIMO: System Overview and Integration," *IEEE/RSJ International Conference on Intelligent Robots and Systems*, vol. 3 (IEEE, 2002) pp. 2478–2483.
[5] J. Y. Kim, J. Lee and J. H. Ho, "Experimental realization of dynamic walking for a human-riding biped robot, HUBO FX-1," *Adv. Rob.* **21**(3–4), 461–484 (2007).
[6] J. Y. Kim, I. W. Park and J. H. Oh, "Experimental realization of dynamic walking of the biped humanoid robot KHR-2 using zero moment point feedback and inertial measurement," *Adv. Rob.* **20**(6), 707–736 (2006).
[7] M. Vukobratoviæ and B. Borovac," Zero-moment point—thirty five years of its life," *Int. J. Hum. Rob.* **1**(1), 157–173 (2004).
[8] C. Hubicki, Energy-Economical Heuristically Based Control of Compass Gait Walking on Stochastically Varying Terrain *Master's thesis* (Bucknell University, 2011).
[9] J. Kennedy and R. Eberhart, "Particle Swarm Optimization," *Proceedings of ICNN'95-International Conference on Neural Networks*, vol. 4 (IEEE, 1995) pp. 1942–1948.
[10] Y. Hürmüzlü and G. D. Moskowitz, "The role of impact in the stability of bipedal locomotion," *Dyn. Stab. Syst.* **1**(3), 217–234 (1986).
[11] T. Anstensrud, 2-D Passive Compass Biped Walker: Analysis and Robustness of Stable Gait *Master's thesis* (Institutt for tekniskky bernetikk, 2013).
[12] M. Mitchell, *An Introduction to Genetic Algorithms* (MIT Press, Cambridge, MA, 1996).
[13] M. Dorigo and G. Di Caro, "Ant Colony Optimization: A New Meta-Heuristic," *Proceedings of the 1999 Congress on Evolutionary Computation-CEC99 (Cat. No. 99TH8406),* vol. 2 (IEEE, 1999) pp. 1470–1477.
[14] M. Reyes-Sierra and C. C. Coello, "Multi-objective particle swarm optimizers: A survey of the state-of-the-art," *Int. J. Comput. Intell. Res.* **2**(3), 287–308 (2006).
[15] M. Preuss, "Niching Methods and Multimodal Optimization Performance," **In:** *Multimodal Optimization by Means of Evolutionary Algorithms* (Springer, Cham, (2015) pp. 115–137.
[16] D. E. Goldberg and J. Richardson, "Genetic Algorithms with Sharing for Multimodal Function Optimization," *Genetic Algorithms and their Applications: Proceedings of the Second International Conference on Genetic Algorithms* (Lawrence Erlbaum, Hillsdale, NJ, 1987) pp. 41–49.
[17] O. J. Mengshoel and D. E. Goldberg, "Probabilistic Crowding: Deterministic Crowding with Probabilistic Replacement," *Proceedings of the Genetic and Evolutionary Computation Conference*, vol. 1 (Morgan Kauffman, 1999) pp. 409–416.
[18] A. Pétrowski, "A Clearing Procedure as a Niching Method for Genetic Algorithms," *Proceedings of IEEE International Conference on Evolutionary Computation* (IEEE, 1996) pp. 798–803.
[19] J. P. Li, M. E. Balazs, G. T. Parks and P. J. Clarkson, "A species conserving genetic algorithm for multimodal function optimization," *Evol. Comput.* **10**(3), 207–234 (2002).
[20] C. Yue, B. Qu and J. Liang, "A multiobjective particle swarm optimizer using ring topology for solving multimodal multiobjective problems," *IEEE Trans. Evol. Comput.* **22**(5), 805–817 (2017).
[21] C. A. C. Coello, G. T. Pulido and M. S. Lechuga, "Handling multiple objectives with particle swarm optimization," *IEEE Trans. Evol. Comput.* **8**(3), 256–279 (2004).

[22] K. Deb, A. Pratap, S. Agarwal and T. Meyarivan, "A fast and elitist multiobjective genetic algorithm: NSGA-II," *IEEE Trans. Evol. Comput.* **6**(2), 182–197 (2002).
[23] J. A. Gallego, A. Forner-Cordero, J. C. Moreno, A. Montellano, E. A. Turowska and J. L. Pons, "Continuous Assessment of Gait Stability in Limit Cycle Walkers," *2010 3rd IEEE RAS & EMBS International Conference on Biomedical Robotics and Biomechatronics* (IEEE, 2010) pp. 734–739.

Cite this article: N. Kim, B. Jeong and K. Park (2022). "A novel methodology to explore the periodic gait of a biped walker under uncertainty using a machine learning algorithm", Robotica **40**, 120–135. https://doi.org/10.1017/S0263574721000424